A non-destructive wind turbine blade analysis based on the Thermal Stress Analysis

Lovre Krstulović-Opara[1], Branko Klarin[1] and Željko Domazet[1]

[1] University of Split, Faculty of Electrical Engineering, Mechanical Engineering and Naval Architecture, R. Boškovića b.b., HR-21000 Split, Croatia

Abstract. In presented paper experimental evaluation of the stress distribution based on the Thermal Stress Analysis has been performed on a wind turbine blade at the second modal vibration regime. Small wind turbine blade was exposed to a simple oscillating movement, similar to the real movement when the blade is mounted on a wind turbine rotor. Internal loads of the blade structure, caused by deflections during oscillated movement, provide energy dissipation in their internal material structure. Energy dissipation, due to the elastic stresses in the structure, can be detected with an infrared thermal imaging camera. The Finite Element modal frequency analysis of the 3D scanned model has been used to evaluate the global structural behaviour and approve Thermal Stress Analysis results. Structure of the blade was detected with ultrasonic probe. As a result, simple procedure for non-destructive structure analysis of the wind turbine blades is proposed.

Keywords*: Thermal Stress Analysis, modal analysis, 3D scanning*

1. Introduction

Often in praxis it comes to the case when existing wind turbine blade has to be evaluated. These are the cases of blades produced by another manufacturer, development of own blades, or production control of own blades. Sometimes it is also good to know what competitors are doing.

The presented work is focused on obtaining the model data of a 600 W wind turbine blade. To evaluate the stress distribution experimental stress evaluation, together with numerical modeling and ultrasonic thickness measurements, has been performed.

To determine the structure and corresponding stress distribution of a vibrating turbine blade, the Thermal Stress Analysis (TSA) has been conducted. The TSA is based on the infrared (IR) camera and Lockin [1]. The Lockin is a hardware component that links thermal image with the load source signal, what together with the software enables better filtering and evaluation of stress distribution images. Due to the basic principles of the TSA, the obtained image represents first invariant of stresses on the body surface [2]. The presented non-destructive method enables obtaining information about the blade structure, eventual delamination, stress

concentration and corresponding critical zones in the geometry of the blade design. It displays critical stress concentration zones, what often does not bring the information about global stress distribution emerging from the blade geometry.

As an additional approval of obtained data, the Finite Element Method (FEM) evaluation has been performed. As the precise model of blade geometry was not known, the 3D scanning of the blade has been performed to obtain CAD model used as the input to the FEM. The conversion of scanned data to the CAD model is the most critical part of the presented approach.

The goal of our research was to leave wind turbine blade intact. As the structure has been unknown, the ultrasonic thickness measurement has been performed, leading to the results confirming TSA.

2. The overview of small wind turbine blades

Blades of small wind turbines can be made of wood or wood composites, aluminum alloys or other light metals, but most common materials are polymer composites (GFK, carbon, aramid etc.).

Like blades designed for large wind turbines, blades for small wind turbines can be designed with shell shaped internal structure, fig.1.a) with strengthening or fig.1.b) without strengthening but with expanded polyurethane foam as the core. Blades can also be made as a compact beam filled with polymer composites stripes on whole cross sectional area, e.g. with no defined internal structure, fig.1.c).

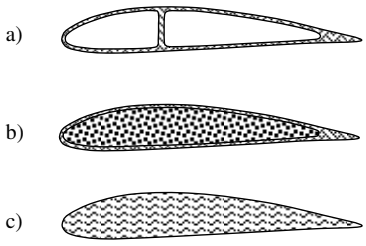

Figure 1. The three main types of the wind turbine blade cross-section:
a) shell shaped internal structure (roving) with strengthening
b) shell shaped blade (roving) with foam core (polyurethane)
c) shaped blade with fully filled structure

The blade of type a) is suitable for large and middle range blades, blade of type b) for middle and small blades, while blade of type c) is appropriate for small and micro wind turbines.

The blade with shaped internal structure a) has better performance, but higher production costs then filled blades b) and c). Filled blades are simpler and cheaper, but with slightly lower performance. Therefore, blades shaped and foam filled b) or fully filled with polymer composites c) are suitable for a mass production of small and micro wind turbines. Figure 2. shows ruptured blade of type b) where internal structure is clearly visible.

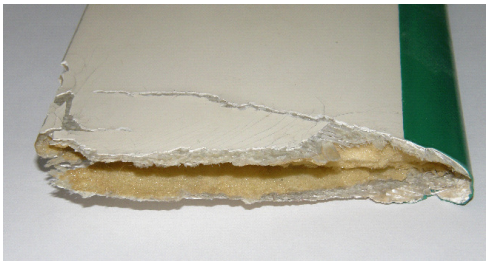

Figure 2. Ruptured wind turbine blade with structure shaped as airfoil (roving mantle), type b). The core is filled out with expanded polyurethane.

In this case (fig. 2) structure has shape of airfoil geometry. The core is filled out with the expanded polyurethane filler of negligible strength properties. Purpose of the filler is to press outer roving mantle (textured fiberglass or carbon fibers) to the both mold sides during the expansion (the blade building process). Thus, light and compact airfoil shaped blade structure can be achieved. On the other hand, figure 3. shows a structure of ruptured blade of type c).

Figure 3. Ruptured wind turbine blade fully filled with fiberglass tapes randomly divided in polymer core, type c).

3. The Thermal Stress Analysis

To perform the TSA, cyclic loading and frequencies above 3 Hz have to be reached. Experimental setup include FLIR SC5000 IR [3] camera with Lockin, accelerometer with amplifier used as a source of signal needed for the TSA, and vibrating frame mechanism with continuous regulation of load frequencies. The Altair-Li software [4] was used for the TSA. The second blade connected with a rigid crosshead has been used to stabilize the system and simulate balanced conditions as it is the case for the rotor setup, fig.4. The frequency of 29.9 Hz, corresponds to second mode of vibrations, what was confirmed with the FEM analysis model (chapter 4.3).

As displacements and corresponding stresses are biggest for the second mode, cycling loading at this frequency exhibits the best thermal effect. Although causing greater displacements and stresses, the first mode is excluded due to the too low frequency for the TSA and instabilities of the vibrating frame mechanism.

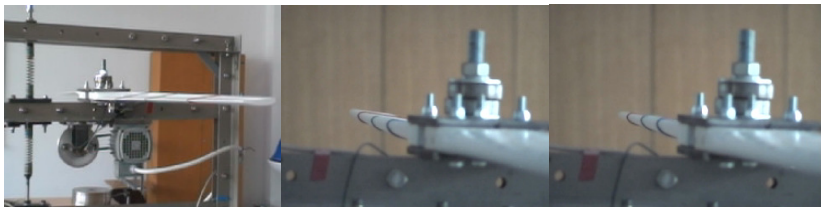

Figure 4. Experimental setup – load frame mechanism and blade vibrations for the 2nd mode.

The blade type is known; shell shaped blade with foam core, or type b) from fig.1. In figure 5. and 6. convex and concave side of wind turbine blade is displayed. The result of the TSA is first stress invariant on the surface, i.e. $\Delta\sigma = \Delta\sigma_1 + \Delta\sigma_2$. For the body surface, the third term of the first invariant does not exist, i.e. $\Delta\sigma_3=0$. To approve the stress concentration zones, ultrasonic thickness gage measurements have been performed.

The thickness analysis showed that the blade is a fiber-glass shell with average thickness of 2.2 mm filled up with the expanded polyurethane foam. While examine regions of stress concentrations (fig. 5 and 6), the ultrasonic thickness analysis approved that the stress concentration is caused by thicker layers of fiber-glass material as a result of production process. These regions, although thicker and with lower stresses, are casing stress concentrations in neighboring transition zones, what represents critical zones where delamination can be initialized.

The reason for different signs of stress values on concave and convex side is the fact that during thermal stress acquisition, the accelerometer was kept on the same side of the blade. As the signal of the accelerometer was used as the source compared with contemporary thermal signal, for one side the thermal image of maximal stresses is in phase with the accelerometer signal, while for another side they are in contra-phase, causing negative signs of stress values. For all figures the stress scale, i.e. the contour scale, was kept constant.

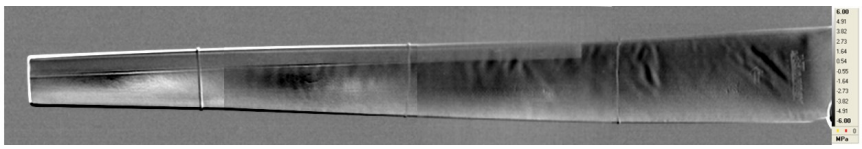

Figure 5. Stress distribution of the convex side of the wind blade.

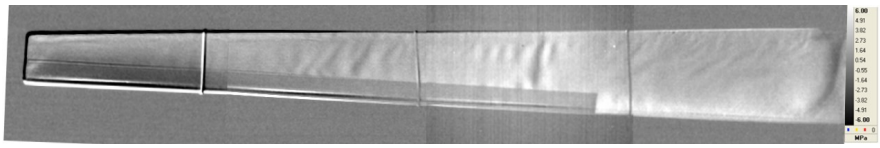

Figure 6. Stress distribution of the concave side of the wind blade.

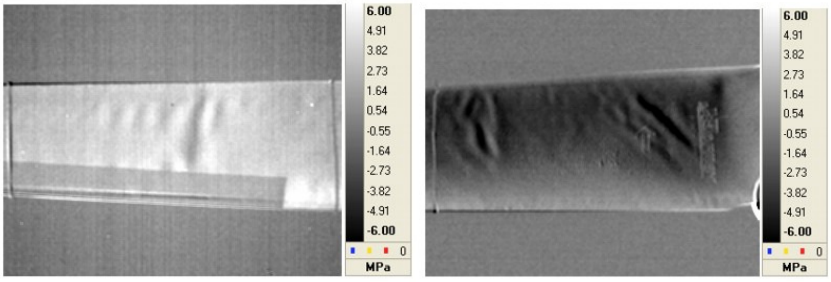

Figure 7. Details of stress concentrations.

Previous figures show irregularities of the blade structure. Such irregularities are typical for the blade of type b). Therefore, the shell shaped structure with foam filled core (polyurethane) is the evaluated blade described in this paper.

Maximal stresses also occurred on the tickets part of the blade, but most exposed are some irregular layers of the roving. These layers are made of irregularly distributed fibers in roving. Irregularities are formed during the shrinkage of the roving fibers. The shrinkage is caused by the expansion of internal polyurethane filament. Due to the friction between fibers and mold surface during high pressure forming caused by the expansion, some fibers are irregularly distributed and shrieked.

Although the blade surface over these layers appears smooth and finished with the high gloss, the layers are characterized by the chaotic and irregular regions that can cause blade damage.

4. The numerical analysis of the scanned geometry

The TSA is a full field method giving the images of the stress distribution on the observed body surface. Often stress concentrations are hiding and interfering with stress distribution caused by the geometry and corresponding loading scenario. Therefore the FEM analysis based on the real wind turbine blade, i.e. the 3D scanned image, is used herein.

4.1. The three dimensional scanning and CAD surface reconstruction

The result of the 3D scanning is a cloud of points, defining the surface more or less accurate. The tedious part of work is obtaining the CAD model, used as a basis for the shell element mesh generation. Shell elements are particularly sensitive to the geometry and element distortions, often causing negative Jacobians and locking. This is not the case for the tetrahedral solid elements.

The wind turbine blade with the trailing edge and curved convex neighboring surface is often tough problem for laser scanners based on the triangulation principle. In our research the wind turbine blade was initially scanned with laser scanner, resulting in uneven blade's trailing edge. The here presented geometry is obtained by the white structured light scanner [5]. Although corresponding CAD surface is

smooth and closed, the CAD patches forming surface could cause problems when exporting IGES data to a FEM code. The presented CAD modeling and FEM analysis was performed using CATIA program package [6].

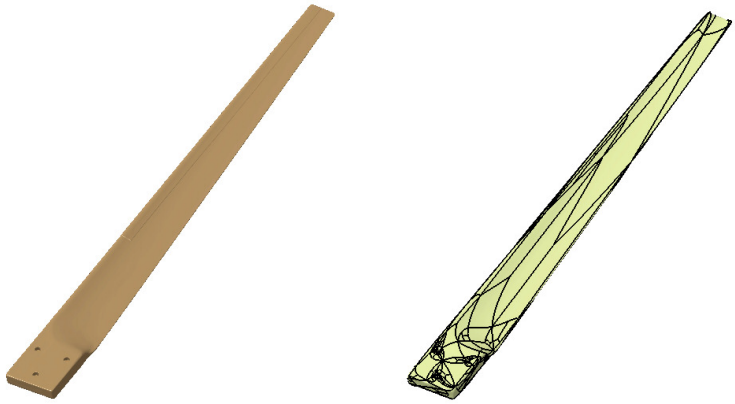

Figure 8. The scanned geometry and reconstructed CAD surface consisting of CAD patches.

4.2. The experimental evaluation of surface thickness

As assumed in [7], to detect the blade's structure, i.e. the fiber-glass thickness, the ultrasonic thickness gage is used. The results for measuring positions are displayed in table 1. Although on the scanned geometry image (STL image) the reinforcement on the blade's leading edge is clearly visible, when constructing the CAD model this information is lost (fig.8). Therefore, a unique thickness of 2.22 mm was adopted for the whole FEM model. This value represents the mean value of measurements displayed in table 1.

Figure 9. The ultrasonic thickness gauge measurement.

Table 1. The thickness at locations of measurements

convex surface	*thickness [mm]*	*concave surface*	*thickness [mm]*
CV1	2.4	CC1	1.1
CV2	0.7	CC2	1.8
CV3	2.3	CC3	1.7
CV4	1.5	CC4	2.6
CV5	2.8	CC5	2.6
CV6	2.8	CC6	**3.9**
CV7	**4.7**	CC7	2.1
CV8	1.6	CC8	2.8
CV9	2.0	CC9	1.4
CV10	1.7	CC10	2.1
CV11	1.7	CC11	2.3
CV12	2.0	CC12	2.4
CV13	**3.9**	CC13	**3.5**

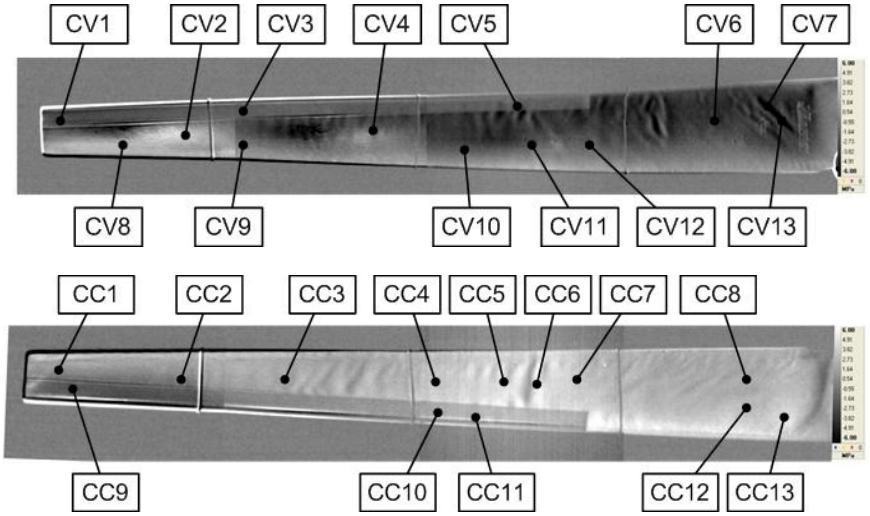

Figure 10. Locations of measurements on convex (CV) and concave (CC) side.

4.3. The FEM analysis

The FEM modal analysis was performed on CATIA package using linear shell elements and linear material model (E=7000 MPa, υ=0.18, $\rho=2.6\cdot10^{-3}$ g/mm^3). The mesh consisted of 6974, mostly quadrilateral shell elements. The blade is clamped on the flat clamping surface, simulating crosshead of the experimental setup.

Modal analysis (table 2) showed the same vibrating mode, i.e. the second mode at the frequency of 36 Hz, what differs from experiment where second mode appeared at 29.9 Hz. The basic difference between the real wind blade and the FEM model is that the polyurethane foam filler was not included in the FEM model. Including damping material as filler to the FEM model would lower resonate frequencies. Figures 8 to 10 depict Von Mises stress distribution of the clamped blade at the second mode.

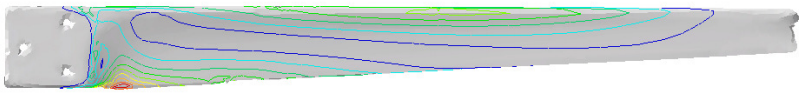

Figure 11. The stress distribution of the concave side of the wind turbine blade.

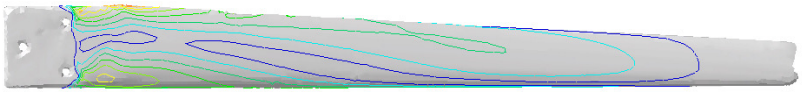

Figure 12. The stress distribution of the convex side of the wind turbine blade.

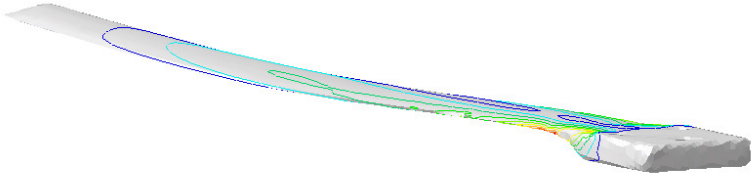

Figure 13. The stress distribution and maximal deformation for 2nd mode of vibrations.

The TSA for the second mode of vibrations mutually confirmed the FEM model, proving that the numerical FEM model as a reliable tool in modeling the behavior of wind turbine blades.

Table 2. Modal frequencies

mode	*frequency*
1	8.01 Hz
2	36.16 Hz
3	40.34 Hz
4	96.88 Hz

A universal non-destructive procedure scheme for long objects based on TSA is depicted in figure 14. Every step of scheme results in assumptions and conclusions, that collected at the end of the procedure represents the synthesis for final conclusion [7].

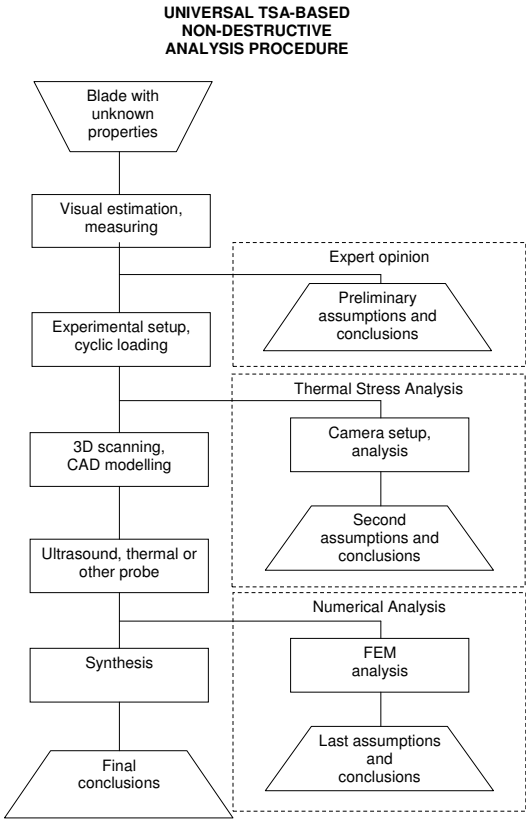

Figure 14. The scheme of a non-destructive analysis procedure based on the TSA, [7].

5. Concluding remarks

The presented approach showed a way how to experimentally and numerically evaluate the existing wind turbine blade. Possibilities and limitations of scanning technologies considering the CAD surface reconstruction are addressed herein.

The development of infrared technologies, with cameras based on the Focal Point Array (FPA) sensors, enabled acquisition at higher frequencies. The infrared equipment and corresponding software represent a reliable and accurate method to determine the stress distribution of cyclically loaded structures. The stress concentration zones, as the main source of fatigue failure, are clearly visible and distinguishable enabling the accurate life time prediction.

As a base of the proposed procedure, the TSA provides experts with assumptions and analysis results even before scanning and modeling the blade. The TSA also helps to make a numerical analysis faster and predictable, without need for extensive iterative investigations, what reduces both time and costs. The proposed procedure of non-destructive analysis provides good basis for a wide range of investigations and eliminates, or reduces, the need of expensive destructive tests.

Acknowledgments

The support from the Ministry of Science, Education and Sports project "Fatigue strength of constructions and materials" and group of Prof. Dr. Željan Lozina is gratefully acknowledged.

References

[1] L.M. Haldorsen. *Thermoelastic stress analysis system developed for industrial applications,* Ph.D. Thesis, University of Aalborg, Institute of mechanical engineering, 1998.

[2] P. Marendić, L. Krstulović-Opara, T. Veljača and Ž. Domazet. *Uvod u termoelastičnu analizu naprezanja*. In P. Marović, M. Galić, L. Krstulović-Opara, editors, *Drugi susreti Hrvatskoga društva za mehaniku,* pages 43-48. Split, 2008.

[3] FLIR SC 5000. http://www.flir.com/thermography/americas/us/content/?id=18356

[4] Altair-Li – FLIR . http://www.flir.com/uploadedFiles/Thermography/MMC/Brochures/1558641/1558641_EN.pdf

[5] ATOS – GOM http://www.gom.com/EN/measuring.systems/atos/system/system.html

[6] CATIA V5R19 – Dassault systems. http://www.3ds.com/products/catia/

[7] L. Krstulović-Opara, Ž. Lozina, B. Klarin: *Mogućnosti postavljanja i primjene nerazornog TSA ispitivanja strukturnih svojstava vjetroturbinske lopatice,* internal study, FESB, Split, 2009.